THERMAL DIFFUSION, AND THERMAL RADIATION EFFECTS ON UNSTEADY MHD CONVECTIVE FLOW PAST AN INCLINED VERTICAL PLATE

N. DAS, S. SARMA and N. AHMED

Department of Mathematics, Gauhati University, Guwahati-14, India.
dasnabanita0825@gmail.com

***Abstract*—– In this investigation, thermal diffusion and thermal radiation effects are studied on an unsteady natural convective flow of an electrically conducting fluid past an inclined vertical plate. A uniform aligned magnetic field is imposed onto the fluid or the plate. The governing PDEs are solved using the Laplace transformation technique. The effect of various parameters on velocity, temperature, concentration, skin friction, Nusselt number, and Sherwood number are analyzed graphically. It is observed that the velocity field rises for increasing the value of the thermal-diffusion effect. Moreover, fluid concentration gets oscillate with the effect of Prandtl number and thermal radiation parameter.**

***Keywords*—– Soret effect, thermal radiation, Inclined plate, Laplace transformation, Roseland approximation.**

I. INTRODUCTION

MHD is the science of motion of electrically conducting fluid in presence of magnetic field. The study of MHD flow is very significant as the topic has diverse applications in various fields of engineering and sciences. MHD principles find numerous applications in missile technology, astrophysics, medical sciences, cosmology, geophysics, etc. Several authors like Alfven (1942), Cowling (1957), Ferraro and Plumpton (1966), Shercliff (1965), Crammer and Pai (1973) made pioneering contributions to the study of MHD. The theoretical significance and the scope of applications of convection problems pertaining to electrically conducting fluid in presence of a magnetic field have received much attention in recent years.

The study of the combined effect of heat and mass transfer on free convection flow received considerable interest in many theoretical models and experimental aspects because of its various applications in industry, scientific, and engineering processes. Some of its applications are in chemical engineering, agricultural engineering, petroleum technology, and many more. The inventive and electrical work of MHD channel flow was studied by Hartmann and Lazarus (1937). The problem concerning MHD free convection and mass transfer flow with heat source and thermal diffusion was studied by Singh (2001). Upreti *et al*. (2022) analyze the nature of heat and mass transfer on the 3D flow of Casson nanofluid. Sharma *et al*. (2007) have studied the Hall effect on MHD mixed convective flow of a viscous incompressible fluid past a vertical porous plate immersed in a porous medium with heat source/sink. Assessment of entropy generation and heat transfer in three-dimensional hybrid nanofluid flow due to convective surface and base fluid were studied by Upreti *et al*. (2021). Heat and mass transfer assessment of magnetic hybrid nanofluid flow via Bidirectional porous surface with volumetric heat generation was examined by Joshi *et al.* (2021). Kim (2001) studied unsteady MHD convection flow of polar fluids past a semi-infinite vertical-moving porous plate in a porous medium. Joshi *et al.* (2015) investigate the mixed convection flow of magnetic hybrid nanofluid over a bidirectional porous surface with internal heat generation and higher-order chemical reaction. Sattar and Hossain (1992) have discussed free convection and mass transfer flow through a porous medium with time-dependent temperature and concentration. Sivaiah *et al.* (2009) and Das and Jana (2015) have studied heat and mass transfer effects on MHD free convection flow with different boundary conditions.

Soret effect which is also known as thermal diffusion effect is concerned with the mass flux under temperature gradient. The experimental investigation of Soret effect was first performed by Swiss chemist Charles Soret in 1879. Soret effect is applied for isotope separation and in a mixture of gas with very light molecular weight (H_2 and H_e). It is observed in mixtures of gases, liquids, and even solids. Several researchers have study on both Soret and Dufour effects due to its various importance. Gamal and Rahman (2010) studied on the Soret and Diffusion thermo effects on Hiemenz flow and mass transfer of fluid flow through a porous medium onto a stretching surface. Turkyilmazoglu and Pop (2012) examined the Soret and heat source effects on the unsteady radiative MHD free convection flow from an impulsively started infinite vertical plate.

Radiation is made of energy transfer in terms of heat by electromagnetic waves or by photons. Thermal radiation on natural convection has become highly significant because of its wide use in Physics and engineering processes. Several authors have investigated the fluid flow with thermal radiation effects. Some of them are Raptis and Perdikis (2003), Makandi (2005), Ahmed and Sengupta (2011), Seth *et al.* (2011), Prasad *et al*. (2021). Omamoke *et al.* (2020) studied the radiation, and heat source effects on MHD free convection flow over an inclined porous plate. Lavanya *et al.* (2020) examine the radiation effect on unsteady free convective MHD flow of a viscous fluid past a porous plate with a heat source. Suresh Babu *et al.* (2021) conduct a numerical study of chemical reaction, diffusion thermos, and radiation effect effects on the unsteady convective flow.

In this paper, our main aim is to study the effects of thermal diffusion and thermal radiation on an unsteady convective flow of an electrically conducting, incompressible fluid past an inclined vertical plate. The flow governing equations are transformed into a non-dimensional form by using non-dimensional parameters. To find the exact solution of the physical model the governed differential equations are solved using a closed from of Laplace transformation technique. Velocity field, temperature field concentration field and skin friction profiles are illustrated graphically. Moreover, heat and mass transfer characteristics are discussed in detail through graphs.

II. MATHEMATICAL FORMULATION

The unsteady motion of an incompressible, viscous, electrically conducting fluid in presence of a magnetic field are governed by the equations

Equation of continuity

$$\vec{\nabla}.\vec{q} = 0 \tag{1}$$

Magnetic field continuity equation

$$\vec{\nabla}.\vec{B} = 0 \tag{2}$$

Ohms law

$$\vec{J} = \sigma\left(\vec{E} + \vec{q} \times \vec{B}\right) = 0 \tag{3}$$

Momentum equation

$$\rho\left[\frac{\partial \vec{q}}{\partial t'} + \left(\vec{q}.\vec{\nabla}\right)\vec{q}\right] = -\vec{\nabla}p + \rho\vec{g} + \vec{J} \times \vec{B} + \mu\nabla^2\vec{q} \tag{4}$$

Energy equation

$$\rho C_p\left[\frac{\partial T}{\partial t'} + \left(\vec{q}.\vec{\nabla}\right)T\right] = \kappa\nabla^2 T - \vec{\nabla}.q_r \tag{5}$$

Species continuity equation

$$\frac{\partial C}{\partial t'} + \left(\vec{q}.\vec{\nabla}\right)C = D_M\nabla^2 C + D_T\nabla^2 T \tag{6}$$

Equation of state on the basis of classical Boussinesq approximation:

$$\rho_\infty = \rho\left[1 + \beta_c(T - T_\infty) + \beta_f(C - C_\infty)\right] \tag{7}$$

Governing equations are based on the work of Ahmed and Sengupta (2011). All the physical quantities involved in the above equations are defined in the list of symbols.

Radiation heat flux as per Suresh Babu *et al.* (2021) approximation

$$\vec{q}_r = -\frac{4\sigma^*}{3\kappa^*}\vec{\nabla}T^4$$

Now, $T^4 = (T - T_\infty + T_\infty)^4 \approx 4T_\infty^3 T - 3T_\infty^3$ as $|T - T_\infty| \ll 1$. So, $\vec{\nabla}\vec{q}_r = -\frac{16\sigma^*}{3\kappa^*}T_\infty^3\nabla^2 T$.

Equation (5) reduces to

$$\rho C_p\left[\frac{\partial T}{\partial t'} + \left(\vec{q}.\vec{\nabla}\right)T\right] = \kappa\nabla^2 T + \frac{16\sigma^*}{3\kappa^*}T_\infty^3\nabla^2 T \tag{8}$$

Introduce a rectangular cartesian coordinate system. The x'- axis is along the plate in the upward vertical direction, the y'-axis taken normal to the imposed aligned magnetic field. Let $\vec{B} = (0, B_0, 0)$ be the magnetic induction vector and $\vec{q} = (u', 0,0)$ be the fluid velocity.

The investigation is restricted to the following assumptions:

(i) All quantities are functions of y' and t'.

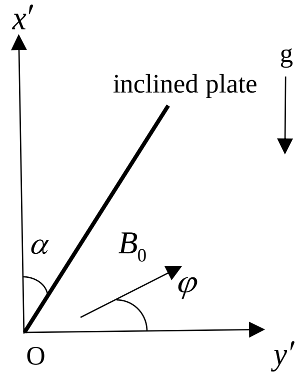

Figure 1: Schematic diagram of the problem

(ii) The Bossinesques approximation, the effect of density fluctuations and species concentration are taken into account.

(iii) Viscous dissipation of energy are negligible.

(iv) Induced magnetic field can be neglected since the magnetic Reynolds number is very small

Equation (4) reduces to

$$\rho\frac{\partial u'}{\partial t'}\hat{\imath} = -\hat{\imath}\frac{\partial p}{\partial x'} - \hat{\jmath}\frac{\partial p}{\partial y'} - B_0^2 u'\sin^2\varphi\hat{\imath} - \rho\mathrm{g}\cos\alpha\hat{\imath} + \mu\frac{\partial^2 u}{\partial y'^2}\hat{\imath} \tag{9}$$

Equation (9) gives

$$\rho\frac{\partial u'}{\partial t'} = -\frac{\partial p}{\partial x'} - B_0^2 u'\sin^2\varphi - \rho\mathrm{g}\cos\alpha + \mu\frac{\partial^2 u}{\partial y'^2} \tag{10}$$

and

$$0 = -\frac{\partial p}{\partial y'} \tag{11}$$

Equation (11) gives the idea that pressure near the plate is equal to the pressure far away from the plate. For fluid region far away from the plate Eq. (10) becomes,

$$0 = -\frac{\partial p}{\partial x'} - \rho_\infty\mathrm{g}\cos\alpha \tag{12}$$

Eliminating $\frac{\partial p}{\partial x'}$, from (10) and (11) we get

$$\rho\frac{\partial u'}{\partial t'} = -\sigma B_0^2 u'\sin^2\varphi - (\rho_\infty - \rho)\mathrm{g}\cos\alpha + \mu\frac{\partial^2 u}{\partial y'^2} \tag{13}$$

Now,

$$\rho_\infty - \rho = \rho\left[\beta_c(T - T_\infty) + \beta_f(C - C_\infty)\right] \tag{14}$$

Putting the value of (14) in the Eq. (13),

$$\rho\frac{\partial u'}{\partial t'} = -\sigma B_0^2 u'\sin^2\varphi - \rho\beta_c(T - T_\infty)\mathrm{g}\cos\alpha + \rho\beta_f(C - C_\infty)\mathrm{g}\cos\alpha + \mu\frac{\partial^2 u}{\partial y'^2} \tag{15}$$

i.e.,

$$\frac{\partial u'}{\partial t'} = \upsilon\frac{\partial^2 u'}{\partial y'^2} + \mathrm{g}\beta_c(C - C_\infty)\cos\alpha + g\beta_f(T - T_\infty)\cos\alpha - \frac{\sigma B_0^2}{\rho}\sin^2\varphi u' \tag{16}$$

Equation (8) becomes

$$\rho C_p\frac{\partial T'}{\partial t'} = k\frac{\partial^2 T}{\partial t'^2} - \frac{\partial q_r}{\partial y'} \tag{17}$$

Equation (6) becomes

$$\frac{\partial C'}{\partial t'} = D_M\frac{\partial^2 C'}{\partial y'^2} + D_T\frac{\partial^2 T}{\partial y'^2} \tag{18}$$

The boundary conditions are

$$t' \le 0: u' = 0, T = T_\infty, C = C_\infty \text{ for all } y$$
$$t' > 0: u' = u_0\exp(a't'), T = T_\infty + (T_W - T_\infty)At',$$
$$C = C_\infty + (C_W - C_\infty)At' \text{ at } y = 0$$
$$u' = 0, T \to T_\infty, C \to C_\infty \text{ as } y \to \infty$$

where

$$A = u_0^2/\upsilon. \tag{19}$$

Introducing non-dimensional quantities,

$$u=\frac{u'}{u_0},\ \theta=\frac{T-T_\infty}{T_W-T_\infty},\ Sc=\frac{\upsilon}{D_M},\ y=\frac{y'u_0}{\upsilon},$$
$$Gr=\frac{g\beta_f\upsilon}{u_0^3}(T_W-T_\infty),\ Gm=\frac{g\beta_c\upsilon}{u_0^3}(C_W-C_\infty),$$
$$Sr=\frac{D_T(T_W-T_\infty)}{\upsilon(C_W-C_\infty)},\ t=\frac{t'u_0^2}{\upsilon},\ \phi=\frac{(C_W-C_\infty)}{(C_W-C_\infty)} \quad (20)$$

Substituting (20) in Eqs. (16)-(18)

$$\frac{\partial u}{\partial t}=\frac{\partial^2 u}{\partial y^2}+Gr\theta\cos\alpha+Gm\phi\cos\alpha-M\sin^2\varphi u \quad (21)$$
$$\frac{\partial\theta}{\partial t}=\frac{1}{\Pr}\left[1+\frac{4}{3N}\right]\frac{\partial^2\theta}{\partial y^2}$$

i.e.

$$\frac{\partial\theta}{\partial y}=\frac{\wedge}{\Pr}\frac{\partial^2\theta}{\partial y^2} \quad (22)$$
$$\frac{\partial\phi}{\partial t}=\frac{1}{Sc}\frac{\partial^2\phi}{\partial y^2}+Sr\frac{\partial^2\theta}{\partial y^2} \quad (23)$$

where $\wedge=\left[1+\frac{4}{3N}\right]$.

Boundary condition

$$t\le 0: u=0,\ \phi=0,\ \theta=0,\ \text{for all } y$$
$$t>0: u=u_0\exp(a_0t),\ \phi=t,\ \theta=t \text{ at } y=0$$
$$u\to 0,\ \theta\to 0,\ \phi\to 0 \text{ as } y\to\infty \quad (24)$$

III. METHOD OF SOLUTION

Taking Laplace transformation of Eqs. (21)-(23), respectively, we get the following ordinary differential equations:

$$s\bar{u}=\frac{\partial^2\bar{u}}{\partial y^2}+Gr\cos\alpha\bar{\theta}+Gm\cos\alpha\bar{\phi}-M\sin^2\varphi\bar{u} \quad (25)$$
$$s\bar{\theta}=\frac{\wedge}{\Pr}\frac{d^2\bar{\theta}}{dy^2} \quad (26)$$
$$s\bar{\phi}=\frac{1}{Sc}\frac{d^2\bar{\phi}}{dy^2}+Sr\frac{d^2\bar{\theta}}{dy^2} \quad (27)$$

Relevant initial and boundary conditions are

$$\bar{u}=\frac{1}{s-a_0},\ \bar{\phi}=\frac{1}{s^2},\ \bar{\theta}=\frac{1}{s^2} \text{ at } y=0$$
$$\bar{u}\to 0,\ \bar{\theta}\to 0,\ \bar{\phi}\to 0 \text{ as } y\to\infty \quad (28)$$

Solving Eqs. from (25)-(27) subject to the initial and boundary conditions (28), we obtain the expression for temperature, concentration, and velocity field as follows

$$\theta=\lambda_1 \quad (29)$$
$$\phi=(1+\eta)\lambda_2-\eta\lambda_1 \quad (30)$$
$$u=\begin{Bmatrix} u_{1,1}+u_{1,2}+u_{1,3}+u_{1,4}: Sc\ne 1,\xi\ne 1, Pr\ne\wedge \\ u_{2,1}+u_{2,2}+u_{2,3}+u_{2,4}: Sc=1,\xi\ne 1, Pr\ne\wedge \\ u_{3,1}+u_{3,2}+u_{3,3}+u_{3,4}: Sc\ne 1,\xi=1, Pr=\wedge \\ u_{4,1}+u_{4,2}+u_{4,3}+u_{4,4}: Sc=1,\xi=1, Pr=\wedge \end{Bmatrix} \quad (31)$$

where,

$$\xi=\frac{\Pr}{\wedge},\ \lambda_1=\lambda(\xi,y,t),\ \eta=\frac{-SrSc\xi}{\xi-Sc},\ a=M\sin^2\varphi,$$
$$\lambda_2=\lambda(Sc,y,t),\ u_{1,1}=u_{1,1,1}-u_{1,1,2}-u_{1,1,3}-u_{1,1,4},$$
$$u_{1,1,1}=\psi_1=\Psi(1,a,a_0,y,t),$$
$$u_{1,1,2}=N_1(A_1\psi_2+A_2\psi_3+A_3f_1),$$
$$N_1=\frac{-Gm\cos\alpha(1+\eta)}{Sc-1},\ A_1=\frac{1}{a_1^2},\ A_2=-A_1,\ A_3=-\frac{1}{a_1},$$
$$\psi_2=\Psi(1,a,a_1,y,t),\ a_1=\frac{1}{Sc-1},\ a_2=\frac{a}{\xi-1},$$
$$\psi_3=\Psi(1,a,y,t),\ f_1=f(1,a,y,t),$$
$$u_{1,1,3}=N_2(A_4\psi_4+A_5\psi_3+A_6f_1),$$
$$N_2=\frac{-Gm\cos\alpha\eta}{\xi-1},\ A_4=\frac{1}{a_2^2},\ A_5=-A_4,\ A_6=\frac{1}{a_2},$$
$$\psi_4=\Psi(1,a,a_2,y,t),\ u_{1,1,4}=N_3(A_4\psi_4+A_5\psi_3+A_6f_1),$$
$$N_3=\frac{-Gr\cos\alpha}{\xi-1},\ u_{1,2}=N_1(A_1\psi_6+A_2\psi_5+A_3f_2),$$
$$\psi_5=\psi(Sc,0,y,t),\ \psi_6=\Psi(Sc,0,a_1,y,t),$$
$$f_2=f(Sc,0,y,t),\ \psi_7=\psi(\xi,0,y,t),$$
$$u_{1,3}=N_2(A_4\psi_8+A_5\psi_7+A_6f_3),$$
$$\Psi_8=\Psi(\xi,0,a_1,y,t),\ f_3=f(\xi,0,y,t),$$
$$u_{1,4}=N_3(A_4\psi_8+A_5\psi_7+A_6f_3),$$
$$u_{2,1}=u_{2,1,1}-u_{2,1,2}-u_{2,1,3}-u_{2,1,4},$$
$$u_{2,1,1}=u_{1,1,1},\ u_{2,1,2}=N_4f_1,\ N_4=\frac{Gm\cos\alpha(1+\eta)}{a},$$
$$u_{2,1,4}=u_{1,1,4},\ u_{2,1,3}=u_{1,1,3},\ u_{2,2}=N_4f_2=u_{4,2},$$
$$u_{2,3}=u_{1,3},\ u_{2,4}=u_{1,4},$$
$$u_{3,1}=u_{3,1,1}-u_{3,1,2}-u_{3,1,3}-u_{3,1,4},\ u_{3,1,1}=u_{1,1,1},$$
$$u_{3,1,2}=u_{1,1,2},\ u_{3,1,3}=N_5f_1,\ N_5=\frac{Gm\cos\alpha\eta}{a},$$
$$u_{3,1,4}=N_6f_2,\ N_6=\frac{Gr\cos\alpha}{a},\ u_{3,3}=N_5f_3=u_{4,3},$$
$$u_{3,4}=N_6f_3=u_{4,4},\ u_{4,1}=u_{4,1,1}-u_{4,1,2}-u_{4,1,3}-u_{4,1,4}$$
$$u_{4,1,1}=u_{1,1,1},\ u_{4,1,2}=u_{2,1,2},$$
$$u_{4,1,3}=u_{3,1,3},\ u_{4,1,4}=u_{3,1,4}$$

Nusselt number

The rate of heat transfer at the plate is given by $Nu=-\left.\frac{\partial\theta}{\partial y}\right]_{y=0}$. Since $\theta=\lambda(\xi,y,t)$ which gives

$$Nu=-v_1 \quad (32)$$

where $v_1=\nu(\xi,t)$.

Sherwood number

Sherwood number is related with the rate of mass transfer at the plate.

$$Sh=-\left[\frac{\partial\phi}{\partial y}\right]_{y=0}=\eta v_1-(1+\eta)v_2 \quad (33)$$

where $v_2=\nu(Sc,t)$.

Skin Friction

The viscous drag is defined in non-dimensional form as, $\tau=-\left.\frac{\partial u}{\partial y}\right]_{\partial y=0}$,

i.e.,

$$\tau=\begin{Bmatrix} \tau_{1,1}+\tau_{1,2}+\tau_{1,3}+\tau_{1,4}: Sc\ne 1,\xi\ne 1, Pr\ne\wedge \\ \tau_{2,1}+\tau_{2,2}+\tau_{2,3}+\tau_{2,4}: Sc=1,\xi\ne 1, Pr\ne\wedge \\ \tau_{3,1}+\tau_{3,2}+\tau_{3,3}+\tau_{3,4}: Sc\ne 1,\xi=1, Pr=\wedge \\ \tau_{4,1}+\tau_{4,2}+\tau_{4,3}+\tau_{4,4}: Sc=1,\xi=1, Pr=\wedge \end{Bmatrix} \quad (34)$$

where

$$\tau_{1,1}=\tau_{1,1,1}-\tau_{1,1,2}-\tau_{1,1,3}-\tau_{1,1,4},$$
$$\tau_{1,1,1}=Z_1=\mathrm{Z}(1,a,a_0,t),\ \Omega_1=\Omega(1,a,t),$$
$$\tau_{1,1,2}=N_1(A_1Z_2+A_2\Omega_1+A_3\Phi_1),$$
$$Z_2=\mathrm{Z}(1,a,a_1,t),\ \Phi_1=\Phi(1,a,t),$$
$$\tau_{1,1,3}=N_2(A_4Z_3+A_5\Omega_1+A_6\Phi_1),$$
$$Z_3=\mathrm{Z}(1,a,a_2,t),\ Z_4=\mathrm{Z}(Sc,0,a_1,t),$$
$$\tau_{1,1,4}=N_3(A_4Z_2+A_5\Omega_1+A_6\Phi_1),$$
$$\tau_{1,2}=N_1(A_1Z_4+A_2\Omega_2+A_3\Phi_2),$$
$$\Phi_2=\Phi(Sc,0,t),\ \Omega_2=\Omega(Sc,0,t),$$
$$\tau_{1,3}=N_2(A_4Z_5+A_5\Omega_3+A_6\Phi_3),$$
$$Z_5=\mathrm{Z}(\xi,0,a_2,t),\ \Omega_3=\Omega(\xi,0,t),\ \Phi_3=\Phi(\xi,0,t),$$
$$\tau_{1,4}=N_3(A_4Z_5+A_5\Omega_3+A_6\Phi_3),$$
$$\tau_{2,1}=\tau_{2,1,1}-\tau_{2,1,2}-\tau_{2,1,3}-\tau_{2,1,4},$$
$$\tau_{2,1,1}=\tau_{1,1,1},\ \tau_{2,1,2}=N_4\Phi_1,\ \tau_{2,1,3}=\tau_{1,1,3},$$
$$\tau_{2,1,4}=\tau_{1,1,4},\ \tau_{2,2}=N_4\Phi_2,\ \tau_{2,3}=\tau_{1,3},\ \tau_{2,4}=\tau_{1,4},$$
$$\tau_{3,1}=\tau_{3,1,1}-\tau_{3,1,2}-\tau_{3,1,3}-\tau_{3,1,4},\ \tau_{3,1,1}=\tau_{1,1,1},$$

$$\tau_{3,1,2} = \tau_{1,1,2}, \tau_{3,1,3} = N_5\Phi_1, \tau_{3,1,4} = N_6\Phi_1, \tau_{3,2} = \tau_{1,2},$$
$$\tau_{3,3} = N_5\Phi_3, \tau_{3,4} = N_6\Phi_3, \tau_{4,1,1} = \tau_{1,1,1},$$
$$\tau_{4,1} = \tau_{4,1,1} - \tau_{4,1,2} - \tau_{4,1,3} - \tau_{4,1,4}, \tau_{4,1,2} = \tau_{2,1,2},$$
$$\tau_{4,1,3} = \tau_{3,1,3}, \tau_{4,1,4} = \tau_{3,1,4}, \tau_{4,2} = \tau_{2,2},$$
$$\tau_{4,3} = \tau_{3,3}, \tau_{4,4} = \tau_{3,4}.$$

IV. RESULTS AND DISCUSSION

To understand the physical depth of the problem, an analytical study has been carried out in the form of graphs. The fluid properties velocity, temperature, concentration, Nusselt number, skin friction, and Sherwood number are illustrated graphically. In most of the cases, the Prandtl number have been kept fixed at 0.71, which corresponds to dry air at 25^0C. Further, the values of thermal Grashof number and solutal Grashof number are chosen to be positive.

The variations of M, Sr, Sc, Gr, Gm and t on velocity field are displayed in Figs. 2-5. It is noticed in Figure 2 that the fluid velocity rises for enhancing the value of Soret number effect. Therefore, the temperature gradient increases fluid velocity rapidly compared to the concentration gradient. Figure 3 represents that the velocity of the fluid increases as the magnetic parameter hikes, *i.e.*, Lorentz force impact the fluid velocity rise. Figures 4 and 5 depicted that fluid velocity falls under the impact of thermal as well as solutal Grashof number. Hence Buoyancy force plays an important role in velocity profile.

Figures 6 and 7 display the effects of thermal radiation N, Prandtl number Pr, and t on temperature distribution. It is observed from Fig. 6 that fluid temperature gets oscillates for raising the value of Pr. It gives the idea that Lower thermal diffusivity oscillates the temperature field inside the boundary layer. Figure 7 represents that by enhancing the value of N, the fluid temperature oscillates inside the boundary layer.

The variation of concentration profile versus y under the effects of Schmidt number Sc, Prandtl number Pr, Soret number Sr, thermal radiation N are represented from Figs. 8-11. Figure 8 suggests that at near the plate the concentration of the fluid shows oscillate behavior with the effect of Sc. But this behavior takes a reverse turn outside the boundary layer. It gives the idea that low mass diffusivity fluctuates the concentration field in a slim layer neighboring the plate. In case of Fig. 9, fluid concentration gives an oscillate behavior in a thin layer for increasing thermal diffusion effect. i.e., higher concentration gradient displays oscillatory behavior inside the boundary layer. Figure 10 and 11 reveals that fluid concentration get oscillate with the effects of thermal radiation parameter N and Prandtl number Pr. It indicates the fact that radiation tends to oscillate concentration of the fluid inside the boundary layer. Similarly, lower thermal diffusivity oscillates the fluid concentration inside the boundary layer.

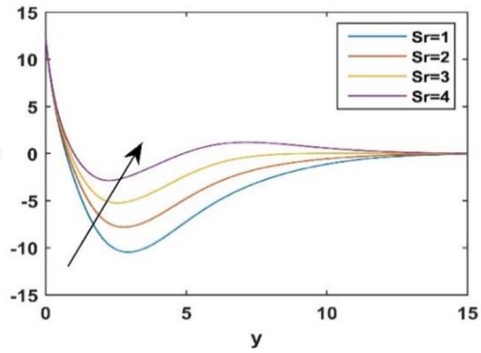

Figure 2: velocity field for the variation in Sr when $M = 1$, $Gr = 15$, $Sc = 0.22$, $t = 0.5$, $Gm = 7$, $\Pr = 0.71$, $\alpha = 60°$, $\varphi = 30°$.

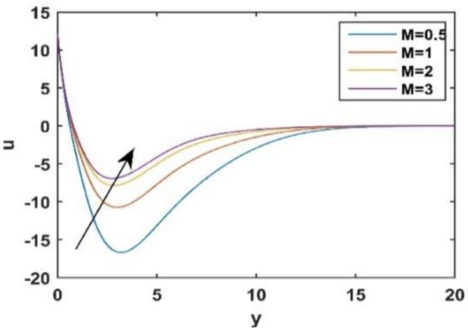

Figure 3: velocity versus y for the variation in M, when $Gm = 7$, $Sr = 1$, $Gr = 15$, $Sc = 0.22$, t=0.5, $\Pr = 0.71$, $\alpha = 60°$, $\varphi = 30°$.

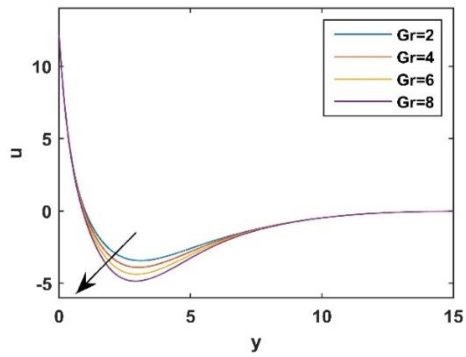

Figure 4: Influence of Gr on velocity profile when $M = 1$, $t = 0.5$, $\Pr = 0.71$, $Gm = 3$, $Sc = 0.22$, $Sr = 1$, $\alpha = 60°$, $\varphi = 30°$.

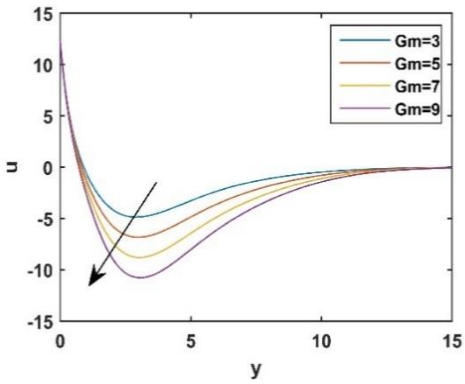

Figure 5: Influence of Gm on velocity when $M = 1$, $Sr = 1$, $Sc = 0.22$, $Gr = 8$, $\alpha = 60°$, $\Pr = 0.71$, $t = 0.5$, $\varphi = 30°$.

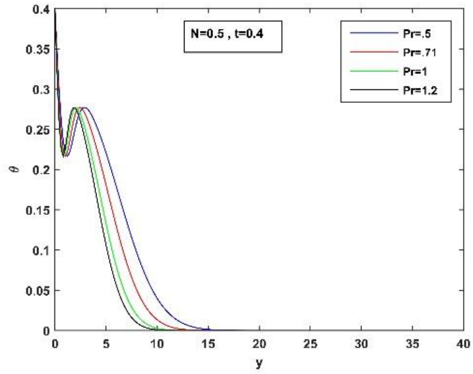

Figure 6: Temperature variation for Pr.

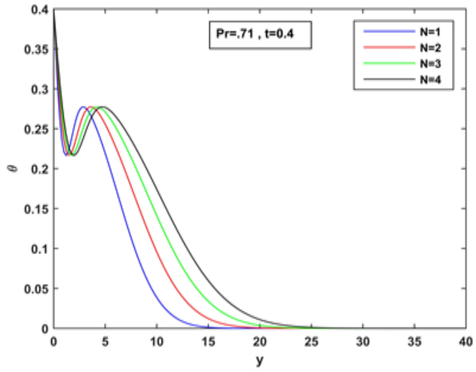

Figure 7: Temperature variation in N.

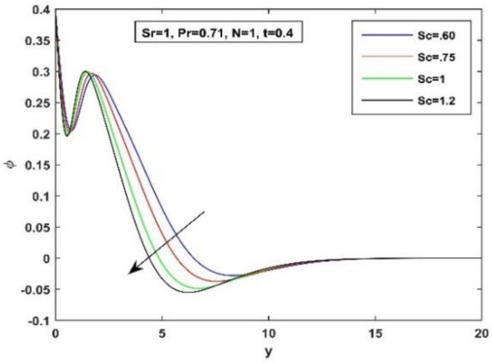

Figure 8: Concentration variation in Sc.

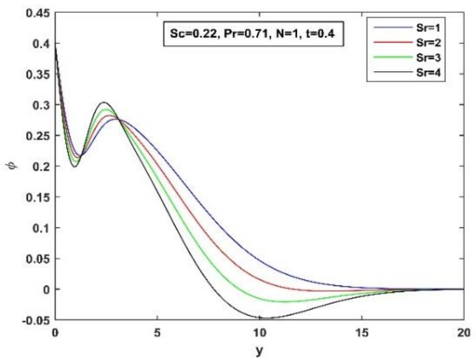

Figure 9: Concentration variation for Sr.

Figures 12-14 explain the variation of viscous drag under thermal diffusion Sr, thermal Grashof number Gr and solutal Grashof number Gm. Figure 12 reveals that the increasing values of Sr, increases the coefficient of

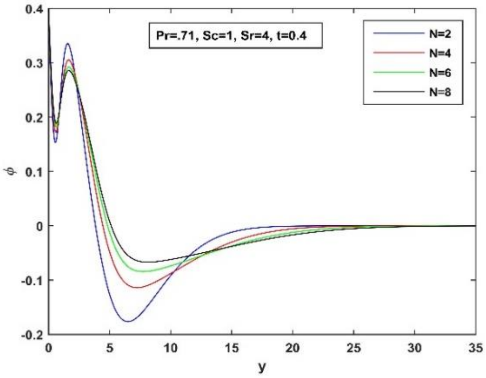

Figure 10: Concentration variation for N.

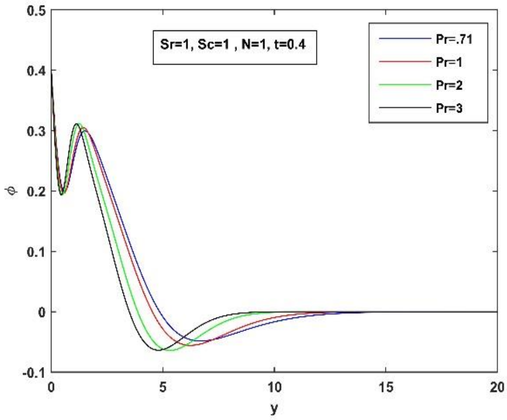

Figure 11: Concentration variation for Pr.

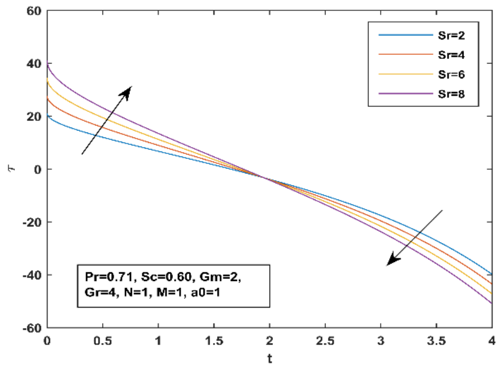

Figure 12: viscous drag versus t for the variation in Sr.

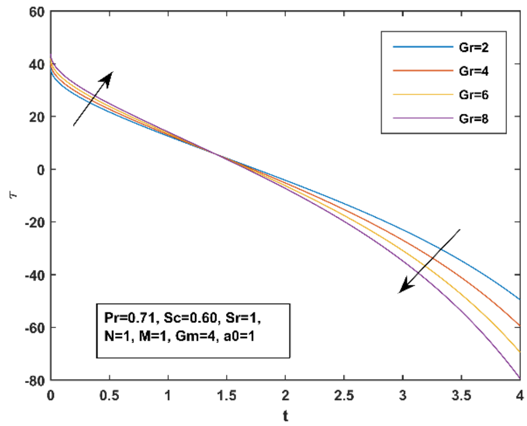

Figure 13: Viscous drag versus t for variation in Gr.

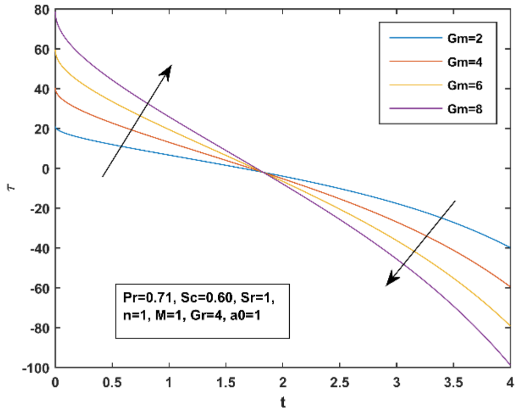

Figure 14: Viscous drag versus t for the variation in Gm.

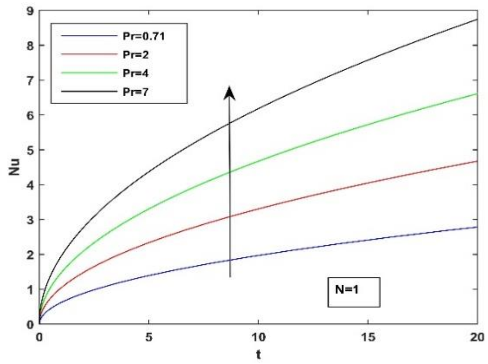

Figure 15: Nusselt number versus t for the variation in Pr.

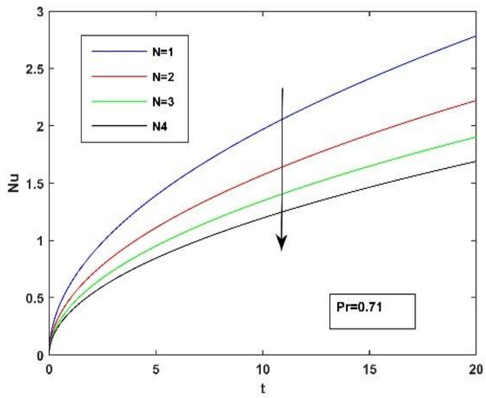

Figure 16: Nusselt number variation in N.

friction for small time and decreases afterwards. Therefore, higher temperature gradient increases rate of momentum transfer for small time and reverses afterwards.Figure 13 and 14 illustrates that Gr as well as Gm increases skin friction for small time, but after a critical point, its nature reverses. So, high thermal buoyancy force and high solutal buoyancy force decreases rate of momentum transfer for small time and increases afterwards.

Figures 15 and 16 exhibits the variation of Nusselt number versus t. Figure 15 shows that there is a comprehensive rise in the Nusselt number with increasing the Prandtl number. $\text{Pr} = 0.71$ represents the value of the Prandtl number in air and $\text{Pr} = 7$ represents the value of

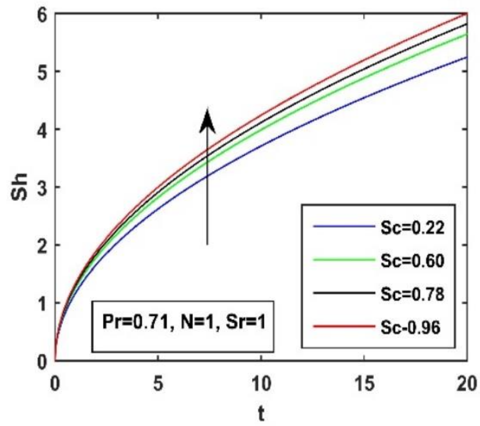

Figure 17: Sherwood number variation in Sc.

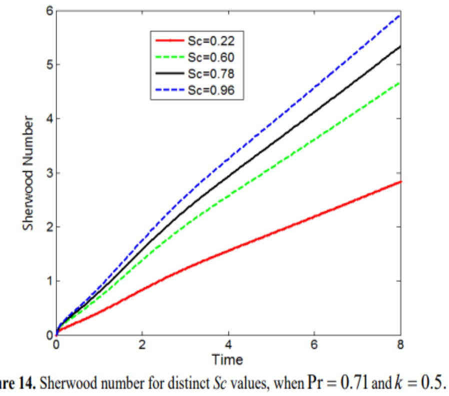

Figure 18: Scanned graph of Sherwood number Profile for different Sc.

the Prandtl number in water. It gives the idea that the rate of heat transfer with a water plate is high compared to air. i.e., lower thermal diffusivity lowers the rate of heat transfer from the plate to the fluid region. Figure 16 admits that the Nusselt number falls with raising the value of N. Therefore, high radiation decreases the rate of heat transfer from the plate to the fluid. The variation of Sherwood number versus t under Sc is displayed in Fig. 17. It is seen that the rate of mass transfer of the fluid rise with the increasing value of both Sc. Figure17 gives us that lower mass diffusivity upsurges the rate of mass transfer from the plate to the fluid.

Comparison of Result

To check the validity of our result, we have compared one of our results with Suresh Babu *et al.* (2021). Figure 17 of our present work and Fig. 18 from the work of Suresh Babu *et al.* (2021) display the Sherwood number profile versus time t for different values of Schmidt number Sc. Both results uniquely established the fact that Sherwood number increases with Schmidt number. Therefore, rate of mass transfer gradually increases under Sc.

V. CONCLUSIONS

The purpose of the present work was to study the effect of thermal diffusion and thermal radiation on an unsteady natural convective flow of an electrically conducting fluid past an inclined vertical plate. A uniform aligned magnetic field is imposed onto the fluid or the plate. The major outcome of the current work is as follows

i. velocity field rise for increasing the value of thermal diffusion effect.
ii. lower thermal diffusivity oscillates the fluid concentration inside the boundary layer.
iii. higher concentration gradient displays oscillatory behavior inside the boundary layer.
iv. high thermal buoyancy force and high solutal buoyancy force increases rate of momentum transfer for small time and decreases afterwards.

The problem is idealized by imposing some realistic constraints. There is a wide scope for reinvesting the same problem numerically by reducing the number of constraints.

NOMENCLATURE

$\vec{B}$ Magnetic flux density vector
Gm Solutal Grashof number
D_M Mass diffusivity(m^2/s)
Gr Thermal Grashof number
Pr Prandtl number
$\vec{E}$ Electric field(V/m)
M Magnetic parameter
D_T Molar thermal diffusivity (J/K·mol)
N Radiation parameter
Sr Soret number
$\vec{J}$ Current density vector(A/m^2)
Sh Sherwood number
C_P Specific heat (at constant pressure) (J/kg. K)
p Pressure(N/m^2)
Sc Schmidt number
t' time (s)
C Concentration (molar species) (mol/m^3)
C_∞ Concentration (far away from the plate)
T_W Wall dimensional temperature (K)
C_s Concentration susceptibility (m^3/kg)
C_w Concentration of the species (at the plate) ($mol/m^{3)}$
a' absorption coefficient
T_∞ Fluid temperature (far away from the plate) (K)
q_r radiative heat flux
g Acceleration (m/s^2)
B_0 Applied magnetic field ($weber/m^2$)
$erfc$ complementary error function

Greek Symbols

ρ Density (kg/m^3)
α angle of inclination.
σ^* Stefan–Boltzmann constant (W/m2 ·K_4)
υ Kinetic viscosity(m^2/s)
κ^* mean absorption constant (1/m)
κ Thermal conductivity (W/m. K)
β_f Volumetric coefficient (thermal expansion) (1/K)
σ Electrical conductivity (s/m)
β_c Volumetric coefficient (solutal expansion) (1/K.mol)
μ Coefficient of viscosity (kg/m. s)
ρ_∞ Fluid density (at free stream) (kg/m^3)

REFERENCES

Ahmed, N. and Sengupta, S. (2011) Thermo-diffusion and diffusion-thermo effects on a three-dimensional MHD mixed convection flow past an infinite vertical porous plate with thermal radiation. *Magnetohydrodynamics*. **47**, 41-60.

Alfven, H. (1942) Discovery of Alfven waves. *Nature*. **150**, 405-406.

Cowling, T.G. (1957) *Magnetohydrodynamic*. Wiley Interscience, New York.

Crammer, K.R. and Pai, S.I. (1973) *Magneto Fluid Dynamics for Engineers and applied physics*. McGraw-Hill Book co. New York.

Das, S. and Jana, R.N. (2015) Natural convective magneto-nanofluid flow and radiative heat transfer past a moving vertical plate. *Alexandria Eng. J.* **54,** 55-64.

Ferraro, V.C.A. and Plumpton, C. (1966) *An Introduction to Magneto-Fluid Mechanics*. Clarendon Press, Oxford.

Gamal, M.A. and Rahman R. (2010) Thermal-diffusion and MHD for Soret and Dufour's effects on Hiemenz flow and mass transfer of fluid flow through porous medium onto a stretching surface. *Physica B Condensed Matter*. **405,** 2560-2569**.**

Hartmann, J. and Lazarus, K. (1937) Kongelige danske videnskabernes selskab. *Matematisk-Fysiske Meddelelser*. **15**, 6-7.

Joshi, N., Pandey, A.K., Upreti, H. and Kumar, M. (2020) Mixed convection flow of magnetic hybrid nanofluid over a bidirectional porous surface with internal heat generation and a higher order chemical reaction. *Heat Transfer*. **50**, 3661-2682.

Joshi, N., Upreti, H., Pandey, A.K. and Kumar, M. (2021) Heat and mass transfer assessment of magnetic hybrid nanofluid flow via Bidirectional porous surface with volumetric heat generation. *International Journal of Applied and Computational Mathematics*. **7**, 64.

Kim, Y.J. (2001) Unsteady MHD convection flow of polar fluids past a semi-infinite vertical-moving porous plate in a porous medium. *International Journal of Heat and mass transfer*. **44,** 2791-2799.

Lavanya, S., Devika, B. and Chenna Kesavaiah, D. (2020) Radiation effect on unsteady free convective MHD flow of a viscoelastic fluid past a tilted porous plate with heat source. *Journal of Xidian University*. **14**, 2298- 2312.

Makinde, O.D. (2005) Free convection flow with thermal radiation and mass transfer past a moving vertical porous plate. *Int. Commun. Heat Mass Transfer*. **32,** 1411-1419.

Omamoke, E., Amos, E. and Bunonyo, K.W. (2020) Radiation and heat source effects on MHD free convection flow over an inclined porous plate in the presence of viscous dissipation. *American Journal of Applied Mathematics*, **8**, 190-206.

Rama Prasad, J.L., Balamurugan, K.S. and Varma, S.V.K. (2021) Aligned magnetic field effect on unsteady MHD double diffusive free convective flow of Kuvshinski fluid past an inclined moving porous plate. *Proceeding of Advances in Fluid dynamics.*

Raptis, A. and Perdikis, C. (2003) Thermal Radiation of an Optically Thin Gray Gas. *International Journal of Applied Mechanics and Engineering*, **8**, 131-134.

Sattar, M.A. and Hossain, M.M. (1992) Unsteady hydromagnetic free convection flow with Hall current and mass transfer along an accelerated porous plate with time-dependent temperature and concentration. *Can. J. Phys.* **70**, 369-374.

Seth, G.S., Ansari, M.S. and Nandkeolyar, R. (2011) MHD natural convection flow with radiative heat transfer past an impulsively moving plate with ramped temperature. *Heat mass transfer*. **47**, 551-561.

Sharma, B.K., Jha, A.K. and Chaudhary, R.C. (2007) Hall effect on MHD mixed convective flow of a viscous incompressible fluid past a vertical porous plate immersed in a porous medium with heat source/sink. *Romanian Journal of Physics.* **52,** 487-503.

Shercliff, J.A. (1965) *A Text Book of Magnetohydrodynamics*. Pergamon Press, London.

Singh, A.K. (2001) MHD free convection and mass transfer flow with heat source and thermal diffusion. *J. of Energy, Heat and Mass Transfer*. **23**, 227–249.

Sivaiah, M., Nagarajan, A.S. and Reddy, P.S. (2009) Heat and mass transfer effects on MHD free convective flow past a vertical porous plate. *The ICFAI University Journal of Computational Mathematics*. **II**, 14-21.

Suresh Babu, R., Thavada, S.K., Venkatachala, G.M., Bandaru, M. (2021) Impact of chemical reaction, Diffusion thermo and Radiation on unsteady Natural convective flow past an inclined vertical plate under aligned magnetic field. *Biointerface research in applied chemistry*. **11,** 13252-13267.

Turkyilmazoglu, M. and Pop, I. (2012) Soret and heat source effects on the unsteady radiative MHD free convection flow from an impulsively started infinite vertical plate. *Int. J. Heat Mass Transfer*. **55**, 7635-7644.

Upreti, H., Pandey, A.K. and Kumar, M. (2021) Assessment of Entropy generation of heat transfer in three-dimensional hybrid nanofluids flow due to convective surfacr and base fluids. *Journal of Porous Media*. **24**, 35-50.

Upreti, H., Pandey, A.K., Uddin, Z. and Kumar, M. (2022) Thermophoressis and Brownian motion effects on 3D flow of Casson nanofluid consisting microorganisms over a Riga plate using PSO: A numerical study. *Chiness journal of Physics*. **78**, 234-270.

APENDIX

Using following functions to solve the problem.

$$\lambda(\xi,y,t)=\left[\left(1+\frac{y^2\xi}{2t}\right)erfc\left(\frac{\sqrt{\xi}y}{2\sqrt{t}}\right)-\frac{\sqrt{\xi}y}{\sqrt{\pi t}}e^{\frac{y^2\xi}{4t}}\right]t,$$

$$f(\xi,\eta,y,t)=\left(\frac{t}{2}+\frac{\sqrt{\xi}y}{4\sqrt{\eta}}\right)e^{y\sqrt{\xi\eta}}erfc\left(\frac{\sqrt{\xi}y}{2\sqrt{t}}+\sqrt{\eta t}\right)+$$

$$\left(\frac{t}{2}-\frac{\sqrt{\xi}y}{4\sqrt{\eta}}\right)e^{-y\sqrt{\xi\eta}}erfc\left(\frac{\sqrt{\xi}y}{2\sqrt{t}}-\sqrt{\eta t}\right),$$

$$\Psi(\xi,\eta,\zeta,y,t)=e^{\zeta t}\psi(\xi,\eta+\zeta,y,t),$$

$$\psi(\xi,\eta,y,t)=\frac{1}{2}e^{y\sqrt{\xi\eta}}erfc\left(\frac{\sqrt{\xi}y}{2\sqrt{t}}+\sqrt{\eta t}\right)+$$

$$\frac{1}{2}e^{-y\sqrt{\xi\eta}}erfc\left(\frac{\sqrt{\xi}y}{2\sqrt{t}}-\sqrt{\eta t}\right),$$

$$\Omega(\xi,\eta,t)=\psi_y^0(\xi,\eta,y,t)=-\left[\frac{\sqrt{\xi}}{\sqrt{\pi t}}e^{-\eta t}+\sqrt{\xi\eta}\,erf\left(\sqrt{\eta t}\right)\right],$$

$$Z(\xi,\eta,\zeta,t)=e^{\zeta t}\Omega(\xi,\eta+\zeta,t)=\Psi_y^0(\xi,\eta,\zeta,y,t),$$

$$\Phi(\xi,\eta,t)=f_y^0(\xi,\eta,y,t)=-\frac{\sqrt{\xi}}{\sqrt{4\eta}}erf\left(\sqrt{\eta t}\right)-$$

$$t\sqrt{\xi\eta}\,erf\left(\sqrt{\eta t}\right)-\frac{\sqrt{t\xi}}{\sqrt{\pi}}e^{-\eta t}.$$

Received: May 17, 2022
Sent to Subject Editor: July 13, 2022 Accepted: January 15, 2023
Recommended by Subject Editor Fabio Giannetti